Surface Reactivity of CF$_2$ Radicals Measured Using Laser-Induced Fluorescence and C$_2$F$_6$ Plasma Molecular Beams

Neil M. Mackie, Vincent A. Venturo, and Ellen R. Fisher*

Department of Chemistry, Colorado State University, Fort Collins, Colorado 80523-1872

Received: July 25, 1997; In Final Form: September 18, 1997[⊗]

The surface reactivity of CF$_2$ radicals during plasma processing of a 300 K Si substrate using the imaging of radicals interacting with surfaces (IRIS) technique is reported. The molecular beam sources are 100% C$_2$F$_6$ and 50:50 C$_2$F$_6$/H$_2$ plasmas. Under IRIS conditions, there is no net film deposition in the former system, while the latter deposits a fluorocarbon polymer film. Simulation of cross-sectional data shows a CF$_2$ surface reactivity of -0.44 ± 0.03 with 100% C$_2$F$_6$ and of 0.16 ± 0.02 using 50:50 C$_2$F$_6$/H$_2$. A negative reactivity indicates CF$_2$ molecules are generated through plasma processing of the substrate. Possible CF$_2$ surface generation mechanisms are discussed.

Introduction

Fluorocarbon discharges have been widely studied because of their dual ability to promote etching of a variety of substrates[1] and to deposit a wide range of fluorinated polymeric films.[2−4] Despite the enormous body of work on plasma etching and deposition using fluorocarbon plasmas (FCPs), details of the mechanisms for both processes remain controversial.[5] Many researchers consider CF$_x$ ($x = 1-3$) radicals as the primary gas-phase precursors for fluorocarbon polymer films deposited from FCPs.[1,6] CF$_x$ radicals are also implicated in plasma etching mechanisms for Si, SiO$_2$, and Si$_3$N$_4$.[7] To clarify mechanistic details, it is necessary to understand the chemical reactions that result when radicals impinge on surfaces during FCP processing.

CF$_2$ radicals are an important CF$_x$ species in FCPs and are postulated to contribute both to plasma polymerization[8] and to selective etching of SiO$_2$.[9] CF$_2$ radicals also help control the concentration of more reactive species such as F radicals,[13] thereby influencing the balance between film deposition and etching in FCPs.[10] To better understand the role of CF$_x$ radicals in FCPs, the gas-phase densities of CF$_x$ species have been measured using mass spectrometry of the effluent gas,[11,12] optical emission actinometry,[6] laser-induced fluorescence (LIF),[13−15] and infrared absorption spectroscopy.[16] In both CF$_4$ and C$_2$F$_6$ plasmas, the CF$_2$ radical density is significant, which has lead many researchers to the conclusion that CF$_2$ contributes to FCP chemistry.[6,10]

Although gas-phase radical densities are important, determining how radicals interact with a substrate is critical to understanding etching and deposition using FCPs. However, few measurements of radical sticking coefficients or surface reactivities are available. Using LIF and a pulsed CF$_4$ radiofrequency (rf) plasma, Booth et al. measured the sticking coefficient, α, of CF$_2$ on Si as ∼0.06.[17] Thoman et al. measured a similar value, $\alpha = 0.02$, on Si using a dc discharge as the source.[18] Using UV laser photolysis, Steinfeld and co-workers examined the mechanism for reaction of CF$_2$ on Si and SiO$_2$ surfaces under UHV conditions.[5] Although no α value was reported, they found CF$_2$ adsorbs on the oxide surface and does not undergo further decomposition. Ion bombardment of the surface resulted in loss of adsorbed CF$_2$ rather than F atom transfer. In contrast, CF$_2$ underwent partial decomposition on

clean Si(100) substrates. Although CF$_2$ radicals have also been observed in various other FCPs,[13−15,19] α values were not reported.

One technique that directly measures the steady-state surface reactivity of a gas-phase species *during* plasma processing is our imaging of radicals interacting with surfaces (IRIS) method.[20,21] IRIS combines molecular beam and plasma technologies with LIF to provide spatially resolved 2D images of radical species involved in film formation or etching. Recent IRIS studies in our laboratory measured the surface reactivity of SiH in SiH$_4$ plasmas,[20] OH in H$_2$O and tetraethoxysilane/O$_2$ plasmas,[20,22,23] and NH$_2$ radicals in NH$_3$ plasmas.[24,25] Here, we present IRIS data for CF$_2$ using a 100% C$_2$F$_6$ plasma and a 50:50 C$_2$F$_6$/H$_2$ plasma as molecular beam sources. The former plasma system is used primarily as a basis for etching plasmas,[26] while the latter deposits amorphous fluorocarbon polymer films.[3,27] In these experiments, we show that the addition of H$_2$ to the feed gas significantly alters the surface reactivity of the CF$_2$ radicals.

Experimental Methods

The IRIS method has been described in detail previously.[11] In a typical IRIS experiment, feed gases enter a glass tube, rf power is applied to an inductor coil, and a plasma is produced. Expansion of the plasma into a differentially pumped vacuum chamber, and ultimately into a high-vacuum region, generates an effusive molecular beam consisting of virtually all species present in the plasma, including the species of interest. A tunable laser beam intersects the molecular beam downstream from the plasma source and excites the radical of choice. Spatially resolved LIF signals are collected by an electronically gated, intensified charge coupled device (ICCD). A substrate is rotated into the path of the molecular beam and LIF signals are again collected. Differences between spatial distributions with the surface in and out of the molecular beam are used to measure a radical's surface reactivity.

In the present work, the source of the molecular beam is a plasma consisting of either 100% C$_2$F$_6$ (Air Products, 99.96%) or a 50:50 mixture of C$_2$F$_6$ and H$_2$ (General Air, 99.95%). Total pressure in the source is 24−26 mTorr for the 100% C$_2$F$_6$ plasma and 28−30 mTorr for the 50:50 C$_2$F$_6$/H$_2$ plasma, as measured by a capacitance manometer. The plasma is produced by the inductive coupling of 13.56 MHz rf power (50 W) and is tuned by an rf matching network.

---

* To whom correspondence should be addressed.
[⊗] Abstract published in *Advance ACS Abstracts,* November 1, 1997.
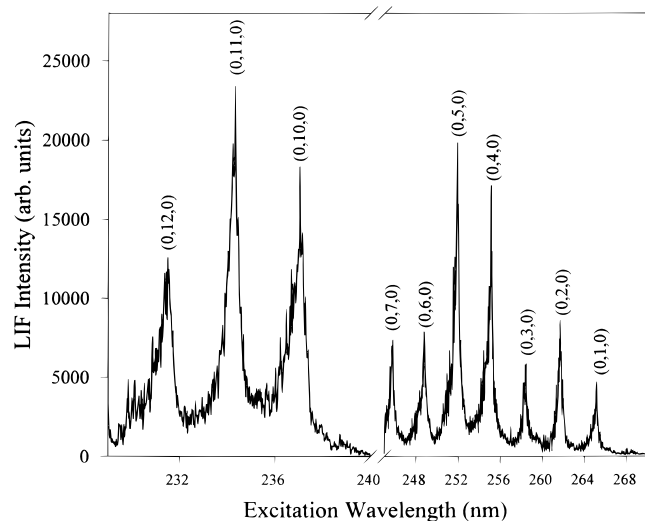
Figure 1. Experimental fluorescence excitation spectrum of CF_2 in a 100% C_2F_6 molecular beam from 229 to 270 nm. The axis break indicates a 5 nm separation between the two dye ranges used, Coumarin 47 (229–240 nm) and Coumarin 307 (245–270 nm). The transition used for all reactivity measurements was the (0,11,0).

The molecular beam was collimated by two slits, 1.03 and 1.30 mm wide, respectively. The slits were mounted on a liquid nitrogen cold shield that was cooled to −200 °C.[24] Tunable laser light in the 229–240 nm range (∼0.3 mJ/pulse) was produced by frequency doubling the output of an excimer-pumped (XeCl, 100 mJ, Hz) dye laser system with Coumarin 47. For the 245–270 nm wavelength range, Coumarin 307 was used. Substrates were 25 × 40 mm p-type silicon (100) wafers with ∼50 Å of native oxide, single polished side facing the molecular beam, placed 2.0 mm away from the laser. No corrections for fluctuations in laser power were made. For the reactivity experiments, LIF from the $A^1A_1(0,11,0)$ state of CF_2 was imaged directly onto the ICCD camera, which has a 586 × 384 pixel display, corresponding to an area of 109 mm². Pixels were binned (4 × 4) to increase signal-to-noise and reduce processing time.

The ICCD camera had a 0.3 μs gate width for the CF_2 molecule (radiative fluorescence lifetime of 61 ± 3 ns).[28] LIF signals were collected for five accumulations of 10–40 s exposure each. Multiple sets of data were taken for each experiment. Background images were taken with the laser tuned to an off-resonance frequency and were subtracted from the data image. A 1D representation of the image was made by averaging 20 columns of pixels (7.74 mm) containing the LIF signal and plotting signal intensity as a function of distance along the laser beam path.

Results and Discussion

Figure 1 shows an excitation spectrum for CF_2 obtained by tuning the laser in 0.025 nm increments from 229 to 240 nm (Coumarin 47, 1 s/step) and from 245 to 270 nm (Coumarin 307 1s/step). Comparison to literature spectra verifies the fluorescing species is indeed CF_2.[28,29] All reactivity data presented here were taken with the laser tuned to the band at 234.323 nm, corresponding to the (0,11,0)−(0,0,0) vibronic band of the CF_2 A^1B_1−X^1A_1 system.

Figure 2 shows a series of ICCD images of CF_2 using a 100% C_2F_6 plasma molecular beam. The LIF signal from CF_2 molecules in the molecular beam only is shown in Figure 2a. Figure 2b is the LIF signal acquired with the substrate rotated into the path of the molecular beam. Here, both the incident and scattered CF_2 molecules are being imaged. Figure 2c is

the difference between Figure 2b and Figure 2a. It is clear from this figure that there is an appreciable amount of CF_2 emanating from the surface.

Figure 3a shows the data of Figure 2 as 1D graphical representations for both the incident molecular beam and for scattered, or desorbed, CF_2 molecules. The broad spatial distribution and the shift of the scattered signal peak maximum away from the incident molecular beam peak maximum indicates the CF_2 radicals scatter with a cosine angular distribution. We can interpret the data shown in Figure 3 with our quantitative model of the experiment,[22,23] which reproduces the scattering data in one dimension. A detailed description of the simulation method is given elsewhere.[23] Briefly, the simulation is based on the known geometry of the experiment and allows for two possible scattering mechanisms, either specular scattering or adsorption−desorption (cosine distribution about the surface normal). To determine the steady-state reactivity of a specific molecule, the fraction of radicals scattering from the surface, S, is adjusted to best fit the experimental data. The surface reactivity, R, is defined as $1 - S$. Also shown in Figure 3 are simulated curves for the incident beam and for scattered molecules assuming an adsorption−desorption mechanism. In Figure 3a, the simulation is shown with $S = 1.44 \pm 0.03$, or $R = -0.44 \pm 0.03$. A negative surface reactivity is possible when the chosen radical is also the volatile product of a surface reaction. Scattering data taken at larger laser-surface distances (5.0 and 7.0 mm) are also well described by cosine distributions.[30] Possible reactions responsible for CF_2 production at the surface are discussed further below.

Figure 3b shows the cross-sectional LIF data for CF_2 using a 50:50 C_2F_6/H_2 plasma molecular beam. Here, the relative intensity of the scattered signal has decreased significantly from the 100% C_2F_6 data. Simulating the 50:50 C_2F_6/H_2 experiment as above yields $S = 0.84 \pm 0.02$, or $R = 0.16 \pm 0.02$, Figure 3b. This is a considerably higher reactivity than was observed with the 100% C_2F_6 plasma molecular beam, Figure 3a. The present results represent the first report of IRIS measurements for any species in fluorocarbon plasma systems.

The most notable aspect of these results is that the steady-state surface reactivity of CF_2 changes significantly with plasma feed gas composition. This is important because it provides insight into the interactions of gas-phase radicals with a surface under different plasma surface modification processes. Although fluorocarbon film deposits from FCPs continually, under etching conditions the polymer film is ablated during plasma processing of a substrate.[31] In our IRIS experiments, we do not observe net film deposition from the 100% C_2F_6 plasma molecular beam.[32] This suggests that the deposition and removal rates for the fluorocarbon adlayer are balanced under these conditions. Our observation of a negative reactivity of the CF_2 molecules ($R = -0.44 \pm 0.03$) in this system indicates that CF_2 must be generated at the surface.

There are several possible routes to production of CF_2 radicals. First, a gas-phase molecule may abstract an adsorbed species to form gas-phase CF_2, such as in reaction 1

$$CF(g) + F(ads) \rightarrow CF_2(g) + * \qquad (1)$$
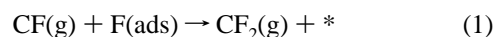
where * represents an adsorption site on the exposed silicon surface. Another possibility is surface decomposition of gas-phase species, such as in reaction 2

$$CF_3(g) + * \rightarrow CF_2(g) + F(ads) \qquad (2)$$
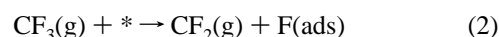
This reaction may contribute greatly to the production of CF_2, since CF_3 radicals are known to dissociate on Si surfaces and

Letters

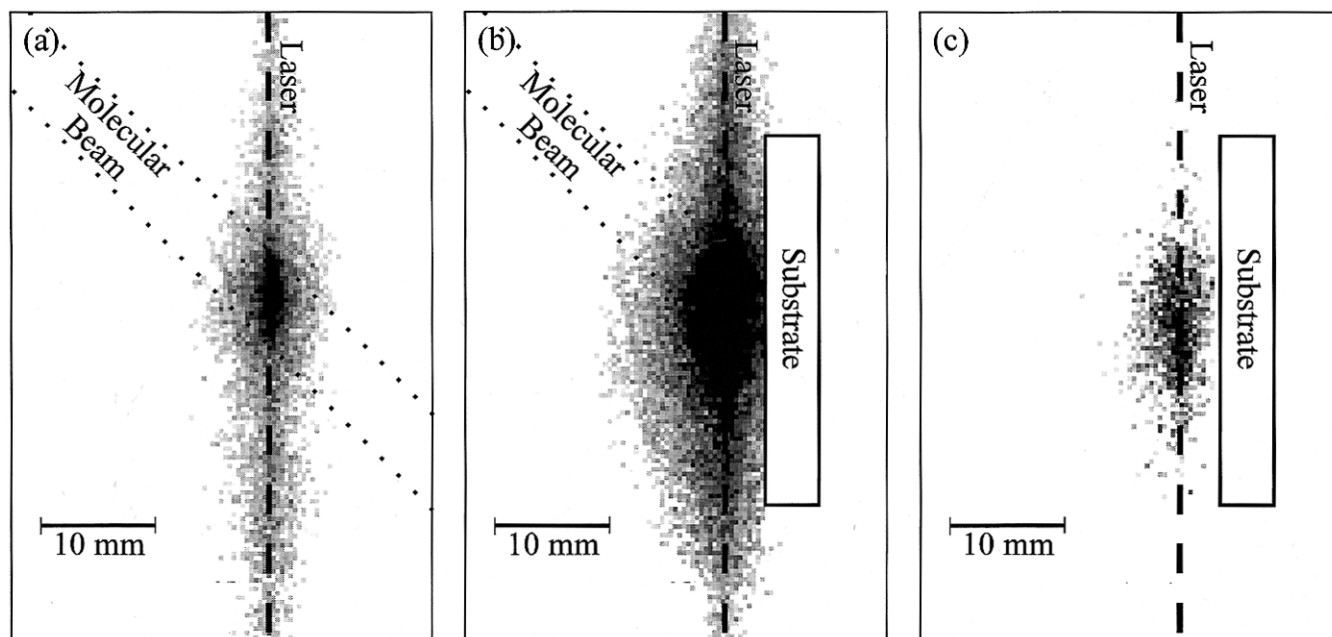*J. Phys. Chem. B, Vol. 101, No. 46, 1997* **9427**

Figure 2. Spatially resolved two-dimensional ICCD images of the LIF signal for the CF_2 (0,11,0) state (a) in the 100% C_2F_6 molecular beam (no substrate) and (b) with a 300 K Si substrate rotated into the path of the molecular beam at a laser−surface distance of 3 mm. (c) Difference between the images shown in (a) and (b) and shows only CF_2 molecules scattering from the surface. LIF signals with the highest intensity appear as the darkest regions in the images. Dashed lines indicate the location of the molecular beam and the laser beam.

on SiO_2 surfaces exposed to ion bombardment.[5,10] Furthermore, the F atom transfer from CF_3 on a Si surface is favored based on thermodynamic arguments.[33]

Another probable source of CF_2 is either physical or chemical sputtering of the fluorocarbon adlayer that is deposited on the surface during plasma processing.[31] Haverlag et al. found that the net CF_2 flux from the rf electrode in a CHF_3 plasma was nearly 2 orders of magnitude higher than the positive ion flux to the electrode.[16] This suggested that physical sputtering was not responsible for the production of CF_2 in this system. Additional experiments demonstrated that chemical sputtering was indeed producing CF_2 at the surface,[16] agreeing with radical/ion beam experiments that indicate the number of radicals chemically sputtered by ions in the presence of fluorine radicals can be much greater than unity.[7,31,34] Thus, chemical sputtering is a likely source of CF_2 generation in our system.

In the 50:50 C_2F_6/H_2 plasma system, an amorphous fluorocarbon film is deposited on the substrate.[3,35] Thus, the addition of H_2 to the plasma shifts the process balance in favor of film formation. The measured R value for CF_2 (0.16 ± 0.02) in this system is significantly higher than the R values measured for 100% C_2F_6 plasmas. This is explained by examining the overall processes occurring in FCPs. The addition of H_2 to a C_2F_6 plasma reduces the F atom concentration since H atoms are F atom scavengers.[6] The loss of F atoms reduces the amount of chemical sputtering that can occur and promotes film deposition over etching. Both of these effects lead to a reduction in surface-generated CF_2. Our observation of $R = 0.16 ± 0.02$ also indicates that CF_2 radicals are consumed at the surface of the growing film. This is consistent with proposed mechanisms that suggest CF_x radicals are building blocks for polymer formation.[6,36] Our results describe the *steady-state* reactivity of CF_2 radicals during fluorocarbon polymer film growth. In IRIS experiments, this measurement involves substrate exposure to the molecular beam for ~150 s or 450 monolayers (of all beam species). This precludes distinction of CF_2 surface reactivities on transient surface compositions that may exist during inital film growth.

The present results can be compared to previous measurements of $\alpha(CF_2)$ on Si surfaces measured by Thoman et al. ($\alpha = 0.02$)[18] and by Booth et al. ($\alpha = 0.06$)[17] in 100% CF_4 plasmas. We find $R = -0.44$ with 100% C_2F_6 and $R = 0.16$ with 50:50 C_2F_6/H_2. There are a number of possible explanations for the observed differences in reactivity. First, there are significant differences in the gas-phase chemistry of CF_4 and C_2F_6 FCPs. CF_4 plasmas have a higher density of F atoms (~2:1) and a higher Si-etch rate,[37] while C_2F_6 plasmas have a higher density of CF_3 radicals.[6,15] Furthermore, CF_2 radicals are produced by different mechanisms in these FCPs.[37]

Differences in the experimental methods for the three investigations are also worth examining. Booth et al. used a parallel plate reactor and modulated the rf power.[17] Pulsed plasmas have steady state densities of both ions and radicals that are considerably altered from continuous wave (CW) plasmas. It has also been shown that radically different film properties and etch profiles can be achieved with pulsed plasmas.[3,38] The significant differences in CF_x radical densities, ion bombardment, and F atom content in this system should be considered when comparing values. Thoman et al. employed a dc discharge source and monitored CF_2 fluorescence downstream from the discharge, 2−15 mm above a Si substrate.[18] While this system is similar to our experimental arrangement, the difference in discharge generation mechanisms (rf vs dc) is likely to produce very different radical distributions.[10,39] Indeed, Thoman et al. observe a significant population in the CF_2 (0,1,0) excited vibrational state. We have attempted to monitor this rovibrational state and do not observe any fluorescence corresponding to excitation from the (0,1,0) state. Interestingly, Thoman et al. also observed net film deposition on Si substrates from their 100% CF_4 plasma, possibly accounting for the positive α value observed.

The present results show that the surface reactivity of CF_2 radicals during plasma processing is strongly dependent on the plasma feed gas composition. Moreover, these experiments demonstrate that gas−surface interactions in FCPs may be strongly affected by plasma type and reactor configuration. The
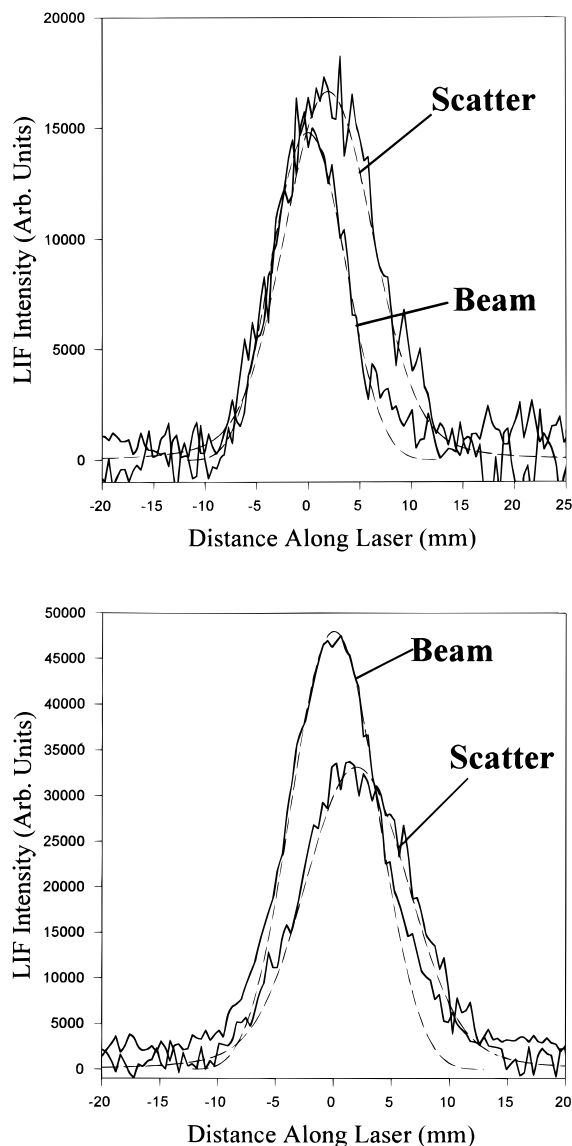
Figure 3. Cross-sectional data for the LIF of CF$_2$ in the incident molecular beam and scattered from a Si (100) substrate using (a, top) a 100% C$_2$F$_6$ plasma molecular beam and (b, bottom) a 50:50 C$_2$F$_6$/H$_2$ plasma molecular beam. The laser surface distances is 2.0 mm. Dashed lines represent the simulated curves from the geometric model assuming (a) $S = 1.44$, adsorption/desorption scattering and (b) $S = 0.84$, adsorption/desorption scattering of CF$_2$.

detailed understanding of radical–surface interactions are vital to the elucidation of deposition and etching mechanisms using fluorocarbon plasmas. Further experiments are currently underway to clarify possible effects of other processing parameters such as substrate material and temperature, alternate plasma feed gases, and rf power modulation.[30]

References and Notes

(1) Kitamura, M.; Akiya, H.; Urisu, T. *J. Vac. Sci. Technol. B* **1989**, *7*, 14–18. Kay, E.; Dilks, A. *Thin Solid Films* **1981**, *78*, 308–318.

(2) Kadono, M.; Inoue, T.; Miyanaga, A.; Yamazaki, S. *Appl. Phys. Lett.* **1992**, *61*, 772–773. d'Agostino, R.; Lamendola, R.; Favia, P.; Giquel, A. *J. Vac. Sci. Technol. A* **1994**, *12*, 308–313. Sah, R. E.; Dishler, B.;

Bubenzer, A.; Koidl, P. *Appl. Phys. Lett.* **1985**, *46*, 739–741.

(3) Mackie, N. M.; Dalleska, N. F.; Castner, D. G.; Fisher, E. R. *Chem. Mater.* **1997**, *9*, 349–362 and references therein.

(4) Golub, M. A.; Wydeven, T.; Finney, L. S. *Plasmas Polym.* **1996**, *1*, 173–194.

(5) Langan, J. G.; Shorter, J. A.; Xin, X.; Joyce, S. A.; Steinfeld, J. I. *Surf. Sci.* **1989**, *207*, 344–353.

(6) d'Agostino, R.; Cramarossa, F.; Fracassi, F.; Illuzzi, F. In *Plasma Deposition, Treatment and Etching of Polymers*; d'Agostino, R., Ed.; Academic Press: San Diego, CA, 1990; pp 95–162.

(7) Miyata, K.; Hori, M.; Goto T. *J. Vac. Sci. Technol. A* **1997**, *15*, 568–572.

(8) Millard, M. M.; Kay, E. *J. Electrochem. Soc.* **1982**, *129*, 160.

(9) Flamm, D. L. *Solid State Technol.* **1979**, *22*, 109.

(10) Lieberman, M. A.; Lichtenberg, A. J. *Principles of Plasma Discharges and Materials Processing*; John Wiley and Sons: New York, 1994.

(11) Hikosaka, Y.; Sugai, H. *Jpn. J. Appl. Phys.* **1993**, *32*, 3040.

(12) Ryan, K. R.; Plumb, I. C. *Plasma Chem. Plasma Process.* **1984**, *4*, 141–146.

(13) Pang, S.; Brueck, S. R. J. *Mater. Res. Soc. Symp. Proc.* **1983**, *17*, 161–168.

(14) Hargis, P. J., Jr.; Kushner, M. J. *Appl. Phys. Lett.* **1982**, *40*, 779–781.

(15) McMillin, B. K.; Zachariah, M. R. *J. Vac. Sci. Technol. A* **1997**, *15*, 230–237.

(16) Haverlag, M.; Stoffels, E.; Stoffels, W. W.; Kroesen, G. M. W.; de Hoog, F. J. *J. Vac. Sci. Technol. A* **1994**, *12*, 3102–3108.

(17) Booth, J. P.; Hancock, G.; Perry, N. D. *Appl. Phys. Lett.* **1987**, *50*, 318. Booth, J. P.; Hancock, G.; Perry, N. D.; Toogood, M. J. *J. Appl. Phys.* **1989**, *66*, 5251.

(18) Thoman, J. W., Jr.; Suzuki, K.; Kable, S. H.; Steinfeld, J. I. *J. Appl. Phys.* **1986**, *60*, 2775–2777.

(19) Ninomiya, K.; Suzuki, K.; Nishimatsu, S.; Okada, O. *J. Vac. Sci. Technol. A* **1986**, *4*, 1791–1794.

(20) McCurdy, P. R.; Bogart, K. H. A.; Dalleska, N. F.; Fisher, E. R. *Rev. Sci. Instrum.* **1997**, *68*, 1684.

(21) Ho, P.; Breiland, W. G.; Buss, R. J. *J. Chem. Phys.* **1989**, *91*, 2627.

(22) Bogart, K. H. A.; Cushing, J. P.; Fisher, E. R. *Chem. Phys. Lett.* **1997**, *267*, 377–383.

(23) Bogart, K. H. A.; Cushing, J. P; Fisher, E. R. *J. Phys. Chem. B*, in press.

(24) McCurdy, P. R.; Venturo, V. A.; Fisher, E. R. *Chem. Phys. Lett.* **1997**, *274*, 120–126.

(25) McCurdy, P. R.; Venturo, V. A.; Fisher, E. R., *J. Phys. Chem.*, in preparation.

(26) Polymer film deposition has been observed with 100% C$_2$F$_6$ when substrates are placed downstream from the visible glow. Castner, D. G.; Lewis, K. B.; Fischer, D. A.; Ratner, B. D.; Gland, J. L. *Langmuir* **1993**, *9*, 537–542.

(27) Ryan, K. R.; Plumb, I. C. *Plasma Chem. Plasma Process.* **1984**, *4*, 271–283.

(28) King, D. S.; Schenck, P. K.; Stephenson, J. C. *J. Mol. Spectrosc.* **1979**, *78*, 1–15.

(29) Matthews, C. W. *Can. J. Phys.* **1967**, *45*, 2355–2374.

(30) Mackie, N. M.; Fisher, E. R. *J. Appl. Phys.*, in preparation.

(31) Ikegami, N.; Ozawa, N.; Miyakawa, Y.; Hirashita, N.; Kanamori, J. *Jpn. J. Appl. Phys.* **1992**, *31*, 2020–2024.

(32) We do observe a small amount of film deposition (<100 Å) if the substrate is processed in the IRIS chamber for a extended period of time (~2–4 h). However, during reactivity measurements (~20 min), there is no observable film deposition from the 100% C$_2$F$_6$ plasma molecular beam.

(33) Steinfeld, J. I. *Chem. Rev.* **1989**, *89*, 1291–1301.

(34) Gray, D. C.; Mohindra, V.; Sawin, H. H. *J. Vac. Sci. Technol. A* **1994**, *12*, 354–364. Gray, D. C.; Tepermeister, I.; Sawin, H. H. *J. Vac. Sci. Technol. B* **1993**, *11*, 1243–1257.

(35) XPS analysis of IRIS substrates indicates the films deposited under these conditions are nearly identical with those deposited directly in the plasma reactor as reported in ref 3.

(36) d'Agostino, R.; Favia, P.; Fracassi, F. *J. Polym. Sci. A: Polym. Chem.* **1990**, *28*, 3387–3402.

(37) d'Agostino, R.; Capezzuto, P.; Bruno, G.; Cramarossa, F. *Pure Appl. Chem.* **1985**, *9*, 1287–1298.

(38) Panchalingam, V.; Chen, X.; Savage, C. R.; Timmons, R. B.; Eberhart, C. *J. Appl. Polym. Sci.: Polym. Symp.* **1994**, *54*, 123–141. Savage, C. R.; Timmons, R. B.; Lin, J. W. In *Structure–Property Relations in Polymers*; ACS Advances in Chemistry Series 240; 1993; pp 745–768.

(39) Morosoff, N. In *Plasma Deposition, Treatment and Etching of Polymers*; d'Agostino, R., Ed.; Academic Press: San Diego, CA, 1990; pp 1–93.